EXPERIMENTAL INVESTIGATION ON THE EFFECT OF DIAPHRAGM IN-PLANE STIFFNESS ON THE SEISMIC RESPONSE OF MASONRY BUILDINGS

Guido Magenes[1], Andrea Penna[2], Ilaria Senaldi[3], Alessandro Galasco[4] and Maria Rota[5]
[1]Associate Professor, University of Pavia, Department of Civil Engineering and Architecture and European Centre for Training and Research in Earthquake Engineering (EUCENTRE), Pavia, Italy, guido.magenes@unipv.it
[2]Assistant Professor, University of Pavia, Department of Civil Engineering and Architecture and EUCENTRE, Pavia, Italy, andrea.penna@unipv.it
[3]Post-doctoral fellow, Department of Civil Engineering and Architecture, University of Pavia, Pavia, Italy, isenaldi@roseschool.it
[4]Post-doctoral researcher, Department of Civil Engineering and Architecture, University of Pavia, Pavia, Italy, alessandro.galasco@eucentre.it
[5]Researcher, EUCENTRE, Pavia, Italy, maria.rota@eucentre.it

ABSTRACT
The influence of the in-plane stiffness of horizontal diaphragms on the global seismic response of masonry buildings is widely recognised as an important issue, which needs to be investigated considering both the scarce availability of experimental data and the capabilities of nonlinear modelling techniques for the analysis of masonry buildings. An experimental program was recently carried out at the EUCENTRE (Italy) aimed at studying the seismic response of double-leaf stone masonry buildings with timber floor and roof in which different levels of strengthening interventions improving diaphragm stiffness and diaphragm-to-wall connections were simulated. Based on the results obtained from experimental shaking table tests, a first series of numerical simulations have been carried out in order to explore the possibility of reproducing the seismic behaviour of the strengthened prototype buildings by means of simplified nonlinear models.

KEYWORDS: masonry buildings, diaphragm stiffness, seismic response, strengthening techniques, nonlinear modelling.

INTRODUCTION
One of the main sources of seismic vulnerability of existing unreinforced masonry buildings is related to the occurrence of failure modes associated to the out-of-plane response of walls. The seismic response could indeed be governed by such mechanisms because of poor connections between orthogonal walls, due to the absence of tie rods or ring beams or by the lack of interlocking between masonry units in correspondence of intersecting walls. In addition, the response of unreinforced masonry structures could be influenced by the in-plane stiffness of diaphragms, which in existing historical masonry construction are typically constituted by simply supported wooden floors and roofs as well as by thin masonry vaults. Flexible diaphragms of such typologies would operate very little coupling effect, hence allowing the vertical structural elements to behave almost independently.

An extended experimental program has been carried out at EUCENTRE Pavia and at the Department of Civil Engineering and Architecture of the University of Pavia, Italy, to analyze

the influence of wall-to-diaphragm connections and diaphragm in-plane stiffness on the seismic performance of undressed double-leaf stone masonry buildings by means of shaking table tests on full-scale prototypes. Three buildings were designed to be one reference structure without any specific antiseismic device and two others where, respectively, lighter and stronger strengthening interventions on diaphragms were applied.

CHARACTERISTICS OF THE TESTED BUILDING PROTOTYPES

The three full-scale stone masonry prototypes share the same geometry, which corresponds to that of a single-room, two storey building with simply supported wooden floor and pitched roof (Figure 1). The longitudinal walls, namely the East and West façades, are oriented in the direction of the uniaxial shaking table motion.

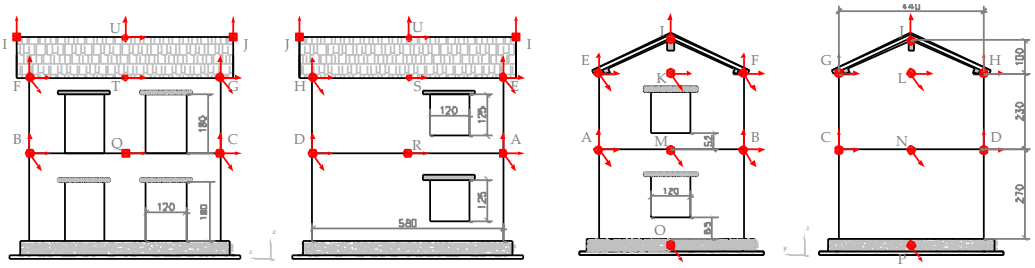

Figure 1 Front views of the walls of the reference geometry and position of the accelerometers installed for the shake table testing (red dots and arrows indicating the monitored dofs).

All specimens were made of double-leaf stone masonry, simulating a typology of historical masonry quite common in Italy, without through stones (apart from corners and vicinity of openings) with a nominal thickness of 32 cm. The two leaves of undressed stones were simply built close to each other with some smaller stones and mortar used to fill the irregular gaps in between. The mechanical properties were determined from simple compression and diagonal compression tests [1, 2], resulting in a mean value of Young's modulus E of 2537 MPa, an average shear modulus G equal to 841 MPa and mean values of vertical compressive strength and diagonal tensile strength respectively of 3.28 and 0.137 MPa. The second and third prototypes are meant to be representative of selected strengthening solutions applied on the reference unstrengthened structure, with the main objective to improve the wall-to-floor connections and to stiffen the floor diaphragms.

In the case of the first prototype building, no strengthening intervention was prearranged until incipient collapse condition was reached because of the activation of an out-of-plane overturning mechanism involving portions of the transverse façades. At that point, in order to guarantee the development of a global response of the structure, a short-term retrofit was activated by post-tensioning steel tie rods, at both levels, and roof pitch bracing steel cables (8mm diameter) cross anchored to the ridge and spreader beams [3].

The enhancement of the connections between walls and diaphragms of the second building prototype was ensured by the realisation of a steel ring beam at the floor level and a reinforced masonry ring beam at the roof level. Floor and roof pitches were stiffened with a second layer of

diagonal cross-planks, which moderately increased the in-plane stiffness, leaving however the possibility of in-plane diaphragm distortion [4].

Based on the results of a research programme carried out at the University of Trento relative to the influence of in-plane floor stiffness [5], the intervention adopted for Building 3 was designed to provide substantial stiffening of the diaphragm at both floor and roof levels. A reinforced concrete ring beam was constructed at roof level and the roof pitches were also stiffened by the application of multilayer spruce plywood panels. A reinforced concrete collaborating slab was added to the original flexible floor, creating a mixed r.c.-wood structure, connected to the walls by external anchoring steel plates and through bars anchored into the concrete slab [6].

SHAKING TABLE TESTS

The strong motion recorded during the 15th April 1979 Montenegro event at the Ulcinj-Hotel Albatros station was selected as reference seismic input to be applied to the prototype buildings during the shaking table tests. The choice of using the same signal for all the dynamic tests allowed monitoring the progressive damage to the structures and comparing the seismic response of the three prototype structures at the same level of nominal intensity of shaking.

The prototype buildings have been subjected to a similar sequence of seismic excitation by gradually increasing the intensity of the ground motion. The reference input was scaled starting from a nominal PGA of 0.05g up to the ultimate limit state of the structure and stopping prior to reaching an incipient collapse condition of the building prototype. The sequence of the dynamic tests performed is presented in Table 1, in which the values of nominal and actual peak table acceleration are summarized for each phase of the testing program. The difference between the nominal PGA and the peak acceleration actually imposed to the structure tested is due to difficulties in the calibration of the shaking table control. As described in detail in [4] and [6], the discrepancy between the reference input signal and the actually imposed motion is evident also when comparing measures of shaking intensity, such as the Cumulative Absolute Velocity and the Housner Intensity at each stage of testing of the three prototypes.

Table 1 Summary of shaking table tests: nominal and actual PGA values.

Test	Building 1		Building 2		Building 3	
	Nominal [g]	Actual [g]	Nominal [g]	Actual [g]	Nominal [g]	Actual [g]
1	0.05	0.07	0.05	0.06	0.05	0.12
2	0.10	0.14	0.10	0.14	0.10	0.27
3	0.20	0.31	0.20	0.26	0.20	0.55
4	0.30	0.50	0.30	0.36	0.30	0.92
5	0.40	0.63	0.40	0.56	0.40	1.28
6	0.40 (TR*)	0.70	0.50	0.71	0.50	1.04
7	-	-	0.60	0.88	0.60	1.49
8	-	-	0.70	1.16	0.30 (AFTS**)	0.66

* TR: test performed after post-tensioning of tie rods. ** AFTS: simulation of an aftershock on a damaged structure.

As evidenced in Table 1, the strengthened prototypes (Buildings 2 and 3) withstood higher levels of shaking intensity before reaching the ultimate limit state in comparison with the unstrengthened Building 1, which attained a near collapse condition at an actual PGA of 0.63g.

EXPERIMENTAL RESULTS FROM SHAKING TABLE TESTS

As emerged from the observation of the shaking table tests performed, the addition of different strengthening interventions to the reference building allowed to enforce a global type of response in Buildings 2 and 3, hence preventing the occurrence of local damage mechanisms, such as the out-of-plane overturning of the upper portions of the transverse façades activated in the case of the first prototype building [3]. In plane failure modes occurred in the masonry piers of the longitudinal walls of Buildings 2 and 3, with prevailing flexural-rocking behaviour exhibited in the West façade and shear failure affecting the squat pier at the base of the East façade, as depicted by the damage patterns recorded at attainment of the ultimate condition (Figure 2) [4,6].

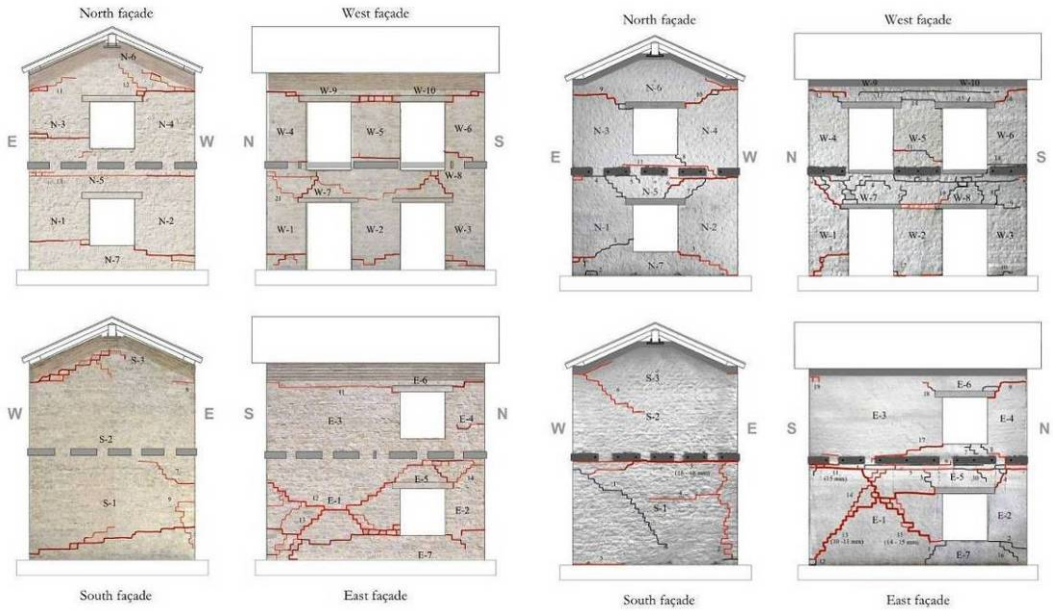

Figure 2 Damage patterns: Building 2 after the test at nominal PGA of 0.70g (left) and Building 3 after the test at nominal PGA of 0.60g (right).

The advanced data acquisition system [7] permitted to monitor and record the displacement demands on the structures, expressed in terms of floor level displacements of the longitudinal walls and of interstorey drifts, which give a further representation of the structural response exhibited at the different stages of testing. The displacements of the longitudinal walls were obtained from the measurements of an optical acquisition system, whereas the transverse components of motion were computed by double-integration of the transverse accelerations [8]. The two floor-level displacements of each longitudinal façade correspond to the average displacement measured at each floor diaphragm. Drifts were evaluated as the ratio of the relative displacement at each floor and the floor height.

The results presented in Table 2 summarizes the maximum displacements in absolute value (Dmax) and maximum interstorey drift, experienced by the three prototypes in correspondence of the opening of the first significant cracks and at the attainment of the ultimate limit state for each building.

The opening of the first significant cracks occurred in correspondence of interstorey drifts between 0.15% and 0.20% for the West façade, within ranges that are consistent with the results obtained from in-plane cyclic tests on masonry piers [2].

Deformed shapes in elevation were produced by plotting the maximum displacement modulus at each floor level, whereas deformed shapes in plan were obtained by plotting the displacements of the walls, at the instant of the occurrence of the maximum displacement, normalized to the maximum component. The nonlinear response of the three structures exhibited at the different stages of the dynamic testing and the damage mechanisms activated are well depicted in both deformed shapes.

Table 2 Summary of maximum absolute displacements and drifts at the opening of first cracks (*cr*) and at the attainment of the ultimate limit state (*u*)

	Building 1				Building 2				Building 3			
	East Wall		West Wall		East Wall		West Wall		East Wall		West Wall	
	Lev.1	Lev. 2	Lev. 1	Lev. 2	Lev. 1	Lev. 2	Lev. 1	Lev. 2	Lev. 1	Lev. 2	Lev. 1	Lev. 2
Nominal (Actual) PGA_cr [g]	0.20 (0.31)				0.40 (0.56)				0.30 (0.92)			
Dmax_cr [mm]	2.2	2.9	3.7	6.6	1.7	3.3	1.7	3.3	2.7	4.4	4.8	9.0
Drift_cr [%]	0.09	0.04	0.15	0.14	0.07	0.07	0.18	0.21	0.11	0.09	0.19	0.17
Nominal (Actual) PGA_u [g]	0.40 (0.63)				0.70 (1.16)				0.60 (1.49)			
Dmax_u [mm]	8	30	21	50	46	67	46	92	32	41	30	50
Drift_u [%]	0.33	0.86	0.82	1.28	1.82	0.89	1.84	2.04	1.29	0.47	1.22	0.78

The three buildings present similar deflected shapes in elevation for the first tests, in which the behaviour is still in the elastic range and the displacements, in the order of few millimetres, show the linear trend typical of a first mode type of response. As expected, once the structure starts behaving inelastically and then reaches an ultimate condition, the deflected shapes reflect the damage mechanism that has developed during the tests. For instance, in the case of the first building prototype during the test at nominal 0.40g, the activation of the out-of-plane overturning mechanism of the upper portion of the transverse walls determines larger drifts at the second floor of the longitudinal walls in comparison to the first level (Figure 3).

In the two strengthened prototype buildings the occurrence of rocking in the slender piers of the West façade and the shear cracks in the East wall determined higher displacement demands at the first storey, as shown in Figure 4 and Figure 5. Furthermore, because of the enhanced wall-to-diaphragm connections and of the increased diaphragm in-plane stiffness, the deformed shapes in plan are characterized by a prevailing uniform translatory motion of the diaphragms (despite some differences at roof gutter level due to the rocking behaviour of the West piers) and rather small components of in-plane angular distortion of floors.

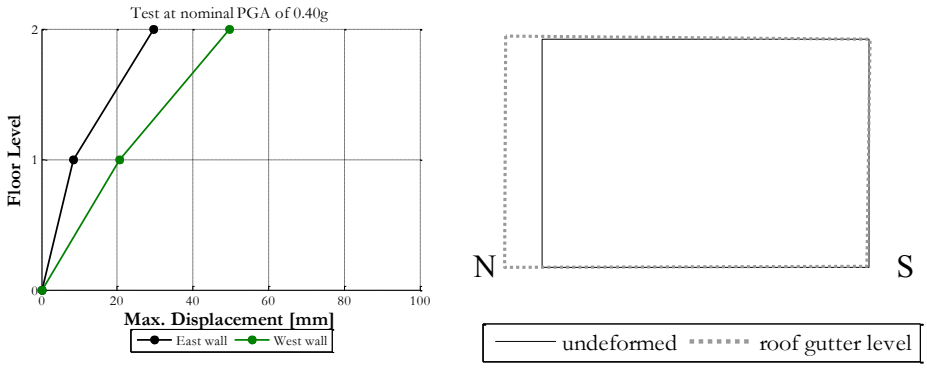

Figure 3 Building 1, test at nominal PGA of 0.40g: deformed shapes in elevation of longitudinal walls (left); deformed shape, plan view (right).

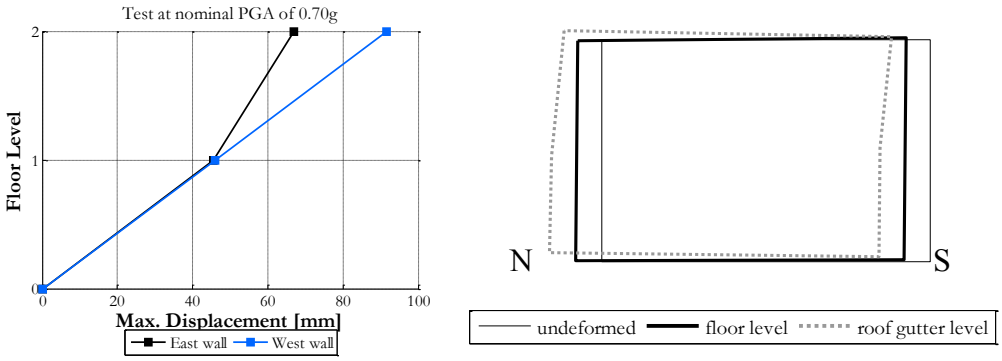

Figure 4 Building 2, test at nominal PGA of 0.70g: deformed shapes in elevation of longitudinal walls (left); deformed shape, plan view (right).

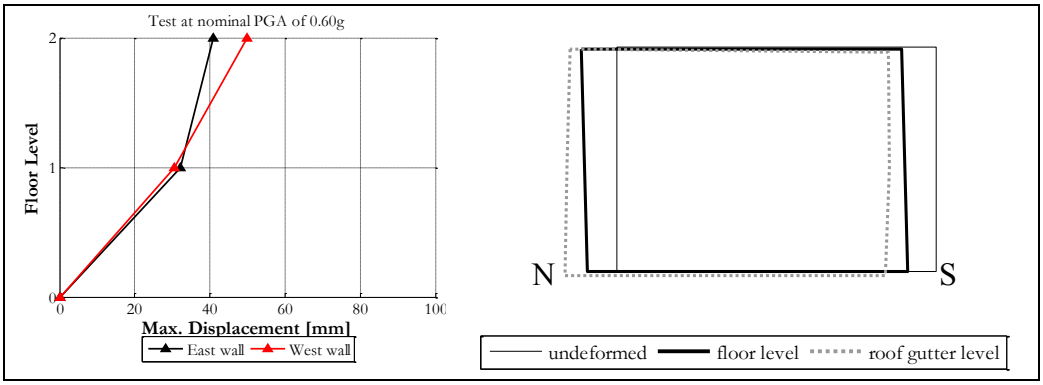

Figure 5 Building 3, test at nominal PGA of 0.60g: deformed shapes in elevation of longitudinal walls (left); deformed shape, plan view (right).

Inertia forces were computed for each building and each dynamic test, as the product of floor and roof level accelerations and tributary masses concentrated at each accelerometer location, and then summed up to produce base shear histories for the whole structure. By making the assumption that half of the inertia forces from each diaphragm are transferred to each longitudinal wall, the base shear for the East and West façades could be separately estimated as well. From the time histories of shear forces at the base and the displacements at top floor (relative to the table), hysteresis curves of the three buildings and of each of the longitudinal

walls were estimated. In Figure 6 the global curves of Buildings 2 and 3 are reported, in which the displacement is the mean of the displacements measured at the roof level in the two longitudinal walls. The shape of the loops is indicative of the hysteretic energy dissipation occurred during each testing phase.

As expected, predominantly linear behaviour is exhibited during the tests in which the structures respond elastically to the seismic input and exhibit minor cracking whereas force-displacement curves start to show a nonlinear behaviour and an increase in hysteretic energy dissipation in correspondence to a moderate cracking of the structural elements. Furthermore, the shapes of the hysteresis loops of the strengthened buildings confirm the visual observations relative to their seismic response. Although both structures experienced similar maximum base shear, the difference among the two in terms of displacement demand is evident.

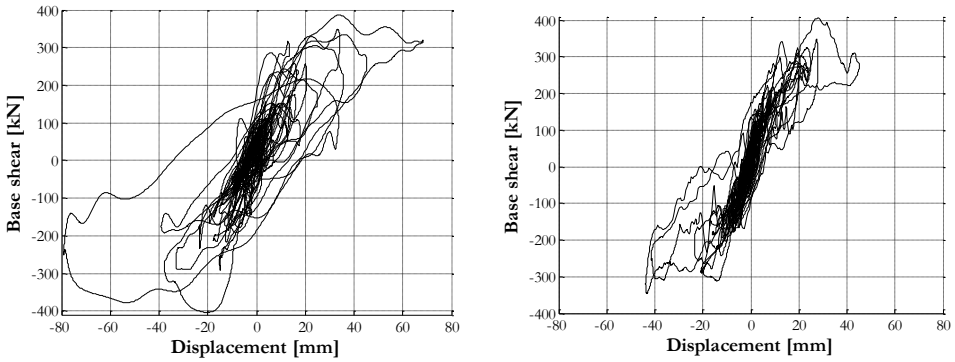

Figure 6 Hysteresis loops: Building 2 during the test at nominal 0.70g (left) and Building 3 during the test at nominal 0.60g (right).

Considering the separate response of the longitudinal walls, the curves in **Error! Reference source not found.** walls confirm the visual observations relative to their seismic response. The slopes of the hysteresis curves depict the differences in stiffness of the longitudinal walls, with the West façade being more flexible than the East wall as expected, as well as the stiffness degradation for increasing level of damage. In **Error! Reference source not found.**, both for Building 2 and for Building 3 for the tests at nominal PGA of 0.60g and of 0.50g respectively, the shape of the curves referred to the West façade is indicative of its prevailing rocking behaviour. While the rocking loops unload with small residual displacement, the loops of the East façade show higher residual displacements and a higher amount of hysteretic energy dissipated, indicative of a higher influence of shear-dominated damage.

The load-bearing capacity and the deformability of the structure usually determine its seismic resistance when subjected to lateral loads. However, the dynamic properties of the structure and the mechanisms activated during strong shaking strongly influence the capability of the structure to absorb and dissipate the induced seismic energy with inelastic deformations [9].

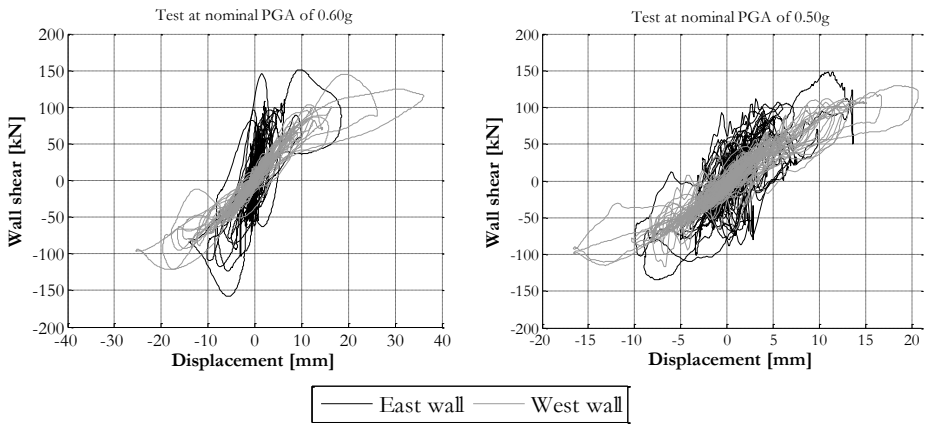

Figure 7 Hysteresis loops of the longitudinal walls: Building 2 during the test at 0.60g (left) and Building 3 during the test at 0.50g (right).

The seismic resistance of the building prototypes has hence been defined through the relationship between the maximum resisted base shear and the corresponding top floor displacement, as an envelope of the hysteresis cycles evaluated during the individual testing phases. Figure 8 shows the plot of the maximum base shear at each stage of testing and the corresponding top floor displacement, occurring at the same instant of time. It should be noted that the last point of each curve (connected by a dotted line to the rest of the curve) is obtained by plotting the maximum displacement, sustained by the structure during the last performed test, and the base shear occurring at the corresponding instant of time.

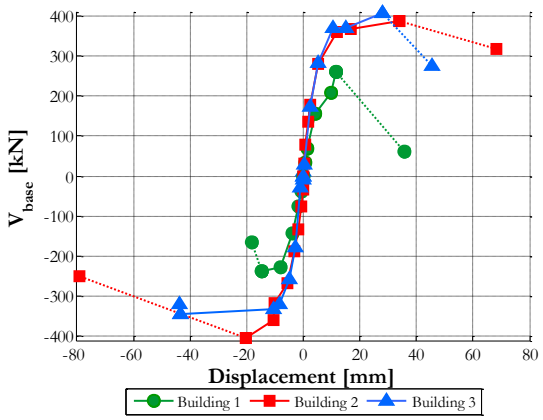

Figure 8 Seismic resistance curves of the three prototypes.

The comparison between the seismic resistance curves of the three buildings showed that the original unstrengthened configuration could withstand much lower levels of shaking intensity with respect to the second and third prototypes that fully exploited the in-plane capacity of the walls. Considering the case of Building 2, in which the wall-to-diaphragm connections were improved maintaining moderately flexible diaphragms, it seems that the major part of the enhancement on the seismic performance is attained, when compared to Building 3: the improvement of the lateral strength capacity and of the performance appears to be related more to the improvement of the floor-to-wall and roof-to-wall connections, which prevented premature out-of-plane failures, rather than to a strong in-plane stiffening of the diaphragms.

NUMERICAL SIMULATION OF THE EXPERIMENTAL RESULTS

Based on the results obtained from the shaking table tests, preliminary numerical models have been developed to reproduce the seismic response exhibited by the two strengthened prototypes during the dynamic tests, by means of nonlinear static analyses.

The two building prototypes have been numerically modelled using an equivalent frame approach, with masonry structural elements defined as nonlinear macro-elements, as proposed by Gambarotta and Lagomarsino [10] and implemented in the program TREMURI [11]. The macro-element model represents the two main in-plane masonry failure modes of a masonry pier or spandrel, bending-rocking and shear-sliding mechanism including friction, with a limited number of degrees of freedom. This model considers, by means of internal variables, the shear damage evolution, which controls the strength deterioration and the stiffness degradation, and rocking mechanism, with toe crushing effect. The shear model implemented in the macro-element is a macroscopic representation of a continuum model [12] in which the parameters are directly correlated to the mechanical properties of the masonry elements. In addition to the geometrical characteristics, the macro-element is defined by six parameters: shear modulus, axial stiffness, masonry shear strength, a non-dimensional coefficient controlling inelastic deformations, global friction coefficient and a factor controlling the softening phase [10]. The macro-element parameters should be considered as representative of an average behaviour of the masonry panel.

The average values of mechanical properties obtained from the masonry characterization test [1] were assigned as macro-element parameters. Diaphragms have been modelled as orthotropic membrane finite elements with four nodes, with mechanical properties defined based on the strengthening interventions on floor and roof diaphragms and on the aforementioned results obtained at the University of Trento [5].

The preliminary discretization of the equivalent frame model was based on the geometry of the prototype buildings, with dimensions of the structural elements defined according to the criteria proposed by Dolce [13]. However, since the preliminary models exhibited a global response that underestimated the experimental behaviour of the structure, in terms of total base shear resisted, and because the geometry (effective height of the piers) of the structural elements is known to influence the damage patterns, the failure mechanisms and consequently the calculated strength and deformation capacity of the systems, the numerical models were refined further modifying the geometry of the piers, as shown in Figure 9.

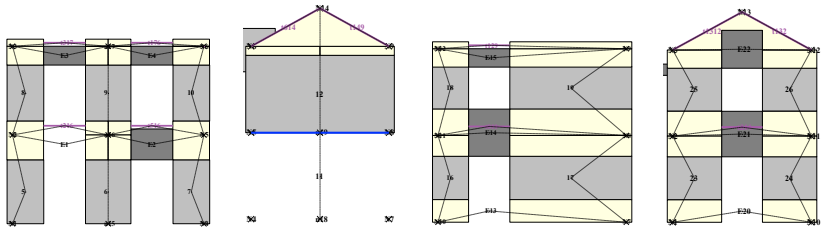

Figure 9 Calibrated discretization of the models, from left: West, South, East and North walls

Nonlinear static analyses were performed subjecting the structures to a modal force pattern. In the experimental dynamic response the measured acceleration profiles were approximately proportional to a first mode of vibration.

The numerical pushover curves are compared with the experimental seismic resistance curves, as shown in Figure 10. The numerical analyses results are in good agreement with the experimental data from the dynamic tests. The calibrated macro-element models approximate fairly well the actual response of the building prototype in terms of maximum resisted shear, with a good agreement of the experimental and numerical curves. The calibrated numerical models depicted fairly well also the damage mechanisms exhibited by the structure during the experimental tests, reproducing the shear failure of the squat pier at the base of the East façade and the rocking type of response of the slender piers in the West façade. It must be pointed out however that the results of the analysis are sensitive to the choices made regarding the effective dimensions of the piers and of the rigid panel zones.

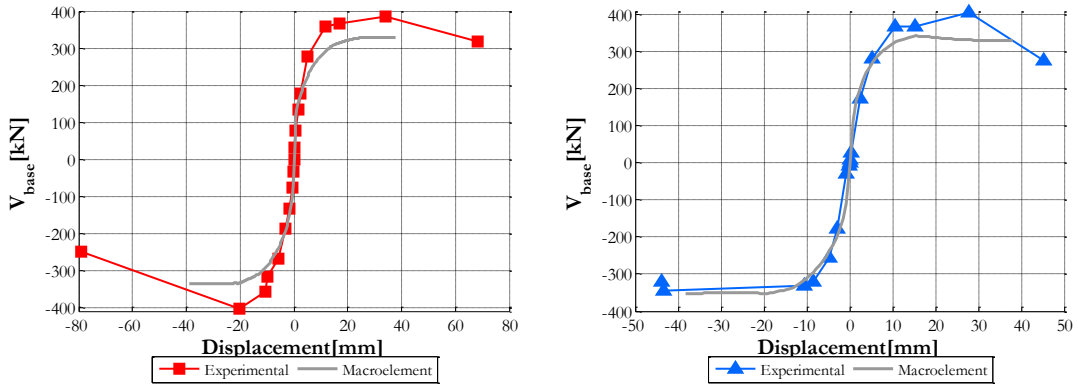

Figure 10 Comparison of numerical and experimental pushover curves: Building 2 (left), Building 3 (right)

CONCLUSIONS

The full-scale shaking table tests performed at EUCENTRE and at the University of Pavia provided valuable results relatively to the seismic response of stone masonry buildings and the effectiveness of selected strengthening strategies. The interventions applied were meant, at different levels, to improve the wall-to-diaphragm connections and to increase the in-plane stiffness of diaphragms and permitted to ensure a global type of response and to prevent the occurrence of out-of-plane local failure mechanisms.

The experimental response of the strengthened prototype buildings was numerically modelled following an existing equivalent frame macro-element approach. In order to better reproduce the experimental behaviour of the structures, both in terms of seismic resistance and of activated damage mechanisms the models have been calibrated modifying the geometry of the structural elements. The numerical simulation showed a significant consistency of the nonlinear static analysis results with the experimental response of the building. Nonetheless, a further integration of the nonlinear static analyses with nonlinear dynamic analyses is needed to reproduce the hysteretic behaviour at levels of acceleration similar to those of the shaking table tests. The calibrated model could then be employed to evaluate the impact of diaphragm stiffening interventions for other configurations of buildings.

ACKNOWLEDGEMENTS

The research project was funded by the Italian Department of Civil Protection, through the Executive Eucentre Project 2005-2008, the 2005-2008 Reluis Project, Line 1 and the 2010-2013 Reluis Project Task AT1-1.1. The authors would also like to thank Tassullo Spa, Rothoblaas Srl and NV Bekaert SA companies, which supported the project. The suggestions of Prof. M. Piazza and Dr. R. Tomasi of the University of Trento and Prof. Modena of the University of Padua are gratefully acknowledged.

REFERENCES

1. Magenes G., Penna, A., Galasco A., Rota M. (2010) Experimental characterisation of stone masonry mechanical properties. In: Proc. 8th International Masonry Conference, Dresden.
2. Magenes G., Galasco A., Penna A., Da Paré M. (2010) In-plane cyclic shear tests of undressed double leaf stone masonry panels. In: Proc. 14th European Conference of Earthquake Engineering, Ohrid.
3. Magenes, G., Penna, A., and Galasco, A., (2010). A full-scale shaking table test on a two storey stone masonry building. In: Proc. 14th European Conference on Earthquake Engineering. Ohrid, Paper no: 1432
4. Magenes, G., Penna, A., Rota M., Galasco, A., and Senaldi, I. (2012). Shaking table test on full-scale stone masonry structures with different strengthening interventions on floor diaphragm. In: Proc. 15th World Conference on Earthquake Engineering. Lisbon, Paper no: 5320
5. Piazza, M., Baldessari, C. and Tomasi, R. (2008). The role of in-plane floor stiffness in the seismic behaviour of traditional buildings. In: Proc. 14th World Conference on Earthquake Engineering. Beijing
6. Magenes, G., Penna, A., Rota M., Galasco, A., and Senaldi, I. (2012). Shaking table test on a strengthened full-scale stone masonry building with flexible diaphragms. In: Proc. 8th International Conference on Structural Analysis of Historical Constructions. Wroclaw, Paper no: 093
7. Lunghi, F., Pavese, A., Peloso, S., Lanese, I., and Silvestri, D. (2012) Role of Seismic Testing Facilities in Performance-Based Earthquake Engineering. Computer Vision System for Monitoring in Dynamic Structural Testing, Springer, pp. 159-176.
8. Boore, D. M. and Bommer, J. J. (2005). Processing of strong-motion accelerograms: needs, options and consequences. Soil Dynamics and Earthquake Engineering 25: 93-115.
9. Tomaževič, M., Weiss, P. and Velechovsky, T. (1991]) The influence of rigidity of floors on the seismic behaviour of old stone-masonry buildings, European Earthquake Engineering 3: 28-41.
10. Gambarotta, L. and Lagomarsino, S. (1996) On dynamic response of masonry panels, Proc. of the National Conference Masonry Mechanics Between Theory and Practice, Messina (in Italian).
11. Galasco, A., Lagomarsino, S., and Penna, A. (2006) TREMURI Program: Seismic Analyzer of 3D Masonry Buildings, University of Genova, Italy.
12. Gambarotta, L., Lagomarsino, S. (1997) Damage model for the seismic response of brick masonry shear walls, Part II: the continuum model and its applications, Earthquake Engineering and Structural Dynamics, Vol. 26, No. 4, pp.423-439.
13. Dolce M. (1991) Schematizzazione e modellazione per azioni nel piano delle pareti, L'Industria delle Costruzioni, Dicembre 1991, 44-57 (in Italian).